NeuroImage 258 (2022) 119345

Contents lists available at ScienceDirect

NeuroImage

journal homepage: www.elsevier.com/locate/neuroimage

Alpha rhythm modulations in the intraparietal sulcus reflect decision signals during item recognition

Sara Spadone, Annalisa Tosoni, Stefania Della Penna[1], Carlo Sestieri[1,*]

Department of Neuroscience, Imaging and Clinical Sciences and ITAB, Institute for Advanced Biomedical Technologies, G. d'Annunzio University of Chieti-Pescara, Room 321, Via dei Vestini 11, Chieti 66100, Italy

ARTICLE INFO

Keywords:
Episodic memory
Decision-making
MEG
Alpha rhythm
Parietal lobe

ABSTRACT

Theoretical work and empirical observations suggest a contribution of regions along the intraparietal sulcus to the process of evidence accumulation during episodic memory retrieval. In the present study, we recorded magnetoencephalographic signals in a group of healthy human participants to test whether the pattern of oscillatory modulations in the lateral parietal lobe is consistent with the mnemonic accumulator hypothesis. To this aim, the dynamic properties and the spatial distribution of MEG oscillatory power modulations were investigated during an item recognition task in which the amount of evidence for old vs. new memory decisions was manipulated across three levels. A data-driven approach was employed to identify brain nodes where oscillatory activity was sensitive to both retrieval success and the amount of evidence for old decisions. The analysis identified three nodes in the left lateral parietal lobe where the event-related desynchronization (ERD) in the alpha frequency band showed both effects. Further analyses revealed that the alpha ERD in the intraparietal sulcus, but not in other parietal nodes: i. showed modulation of duration in response to the amount of evidence for both old and new decisions, ii. was behaviorally significant, and iii. more accurately tracked the subjective memory judgment rather than the objective memory status. The present findings provide support for a recent anatomical-functional model of the parietal involvement in episodic memory retrieval and suggest that the alpha ERD in the intraparietal sulcus might represent a neural signature of the evidence accumulation process during simple memory-based decisions.

1. Introduction

Several lines of evidence support the presence of a functional subdivision in the posterior parietal cortex (PPC) during memory retrieval: ventral parietal regions, such as the angular gyrus (AG), have been associated with the representation of retrieved events, whereas dorsal parietal regions along the intraparietal sulcus (IPS) are thought to contribute to the use of retrieved information for the current goals (Sestieri et al., 2017, see also Vilberg and Rugg (2008)). A specific hypothesis, based on theoretical models (see Ratcliff 1978) and empirical observations (e.g., Kahn et al. 2004, Wheeler and Buckner 2003), further proposes that regions of the IPS might serve as a mnemonic accumulator of evidence for memory-based decisions (Sestieri et al., 2017; Wagner et al., 2005), in analogy with the mechanism of evidence accumulation for perceptual decisions described in classical neurophysiological work (reviewed in Gold and Shadlen (2007)). In line with this hypothesis, fMRI studies have shown that activity in the IPS tracks decision evidence and predicts the subject's choices during item recognition (Guidotti et al., 2020; Sestieri et al., 2014) and source memory (Guidotti et al., 2019) decisions. However, the mnemonic accumulator hypothesis is based almost exclusively on the pattern of BOLD response, which has poor temporal resolution and reflects the sum of hemodynamic activity related to multiple processes.

The EEG literature has consistently described a retrieval-related ERP component in left posterior electrodes with a latency of ~500 ms from the stimulus onset (reviewed in Rugg and Curran (2007), Staresina and Wimber (2019)), but the limited spatial resolution of the technique has not allowed to connect this finding with the fMRI literature. An alternative strategy to test and assign a neurophysiological signature to the mnemonic accumulator hypothesis is the analysis of MEG oscillatory activity. Most prior studies have focused on the role of event-related synchronization (ERS) in the theta (4–7 Hz) and gamma (> 40 Hz) frequency bands as a possible neural mechanism mediating the reinstatement of the original memory trace (Nyhus and Curran, 2010; Staresina and Wimber, 2019; Staudigl and Hanslmayr, 2013). However, these modulations (e.g., Osipova et al. 2006) do not appear to match the

* Corresponding author.
E-mail address: c.sestieri@unich.it (C. Sestieri).
[1] These authors contributed equally to this work.

https://doi.org/10.1016/j.neuroimage.2022.119345.
Received 27 December 2021; Received in revised form 14 May 2022; Accepted 30 May 2022
Available online 31 May 2022.

topography of the fMRI retrieval-related activity, making it difficult to draw a coherent picture. More recently, there has been a renewed interest in the role of event-related desynchronization (ERD) in the alpha (8–13 Hz) band (Griffiths et al., 2019; Karlsson et al., 2020; Sutterer et al., 2019). One study has further demonstrated a spatial overlap between the retrieval-related activity recorded through MEG and fMRI (Martin-Buro et al., 2020) and proposed a role for alpha ERD in the accumulation of mnemonic evidence, implying a functional analogy with the fMRI results.

In the present study, we more directly tested whether oscillatory activity in PPC reflects decision-related processes during memory retrieval. To this aim, we investigated the temporal properties and the spatial distribution of MEG oscillatory power modulations during an item recognition paradigm that manipulates the amount of evidence for old and new decisions (Guidotti et al., 2020; Sestieri et al., 2014). A whole-brain analysis identified regions where the frequency-specific oscillatory power modulations were sensitive to both retrieval success (Hanslmayr et al., 2012; Nyhus and Curran, 2010) and the amount of evidence for old decisions, a potential neural signature of the mnemonic accumulation process. Notably, we opted for a data-driven approach as it provides unique information about the spatial selectivity of the observed modulations. Further analyses examined the role of the identified nodes in the representation of a decision variable. Specifically, we tested whether the evidence modulation identified in old trials was also present for new responses and whether it was explained by a difference in ERD/ERS temporal dynamics indexing processing time (Spadone et al., 2021a), which can be linked to decision-related processes. Specifically, based on the prediction of drift-diffusion models applied to item recognition decisions (Ratcliff, 1978), the accumulation of evidence for old or new decisions is supposed to be slower, and the decision bound to be reached later, for low evidence trials compared to high evidence trials. Following our assumption about the link between alpha ERD and the computation of a decision variable, this should be reflected in a more prolonged alpha ERD for low evidence trials. Moreover, based on the hypothesis that decision-related activity is crucial for task performance, we tested whether the oscillatory power modulation showed a significant relationship with item recognition accuracy across subjects. Finally, we employed a within-subject classification approach to examine the extent to which the pattern of ERD/ERS tracked the subjective choice rather than the objective memory status, as this would support a role in the subjective judgment rather than in the actual recovery of information about the item (Kahn et al., 2004; Wheeler and Buckner, 2003). We identified a node in the IPS showing a pattern of alpha ERD that might represent a spectral signature of evidence accumulation during memory-based decisions.

2. Methods

2.1. Participants

A group of 26 healthy, right-handed participants (16 females, mean age: 25 years) participated in the study. Participants were recruited among students of the University G. d'Annunzio of Chieti-Pescara and were naïve as to the purpose of the experiment. The study was conducted in accordance with the ethical standards of the 1964 Declaration of Helsinki and was approved by the University Ethics Committee. Four subjects were excluded from the analyses based on the poor quality of the MEG recordings ($N = 1$), lack of a sufficient number of brain IC after ICA decompositions ($N = 2$), and technical problems during MEG acquisition ($N = 1$).

2.2. Procedure

The experiment involved two sessions (encoding and retrieval) performed on consecutive days in a magnetically shielded room. The average interval between the retrieval and the encoding session across subjects was 16 h and 45 m (+/- 18 m). MEG signals were only recorded during the retrieval session.

2.2.1. Evidence manipulation

Decision-making is based on the amount of information favoring one of the possible choice options, which can be defined as decision evidence. According to influential drift-diffusion models, decisions can be described in terms of a diffusion process in which a decision variable gradually drifts toward a bound indicating one of two choices (Smith and Ratcliff, 2004). When applied to old/new decisions, these models depict item recognition as a process of accumulation of a relatedness value or "resonance" about the number of features shared by the probe and the items included in the memory set (Ratcliff, 1978; Ratcliff et al., 2004). As in previous work (Guidotti et al., 2020; Sestieri et al., 2014), the amount of evidence favoring "old" decisions was manipulated in the present study by varying the number of times (1, 3, 5) an individual picture was shown during the encoding session (i.e., encoding strength, see Fig. 1A). The underlying assumption is that the more an item is repeated at encoding, the more is the evidence for an old decision at retrieval (i.e., better match between the probe and the memory item) which is typically manifested in better task performance. We also manipulated the amount of evidence for "new" decisions by varying the similarity between old and new images, under the assumption that a higher distinctiveness of the new items provides increasing evidence for a new decision (worse match between the probe and the items in the memory set). While the present paradigm made use of a fixed delay between the onset of the stimulus and the motor response, a procedure that allows separating decision-related from motor-related activity but prevents from calculating the model parameters, the manipulation has been shown to specifically affect the process of evidence accumulation in a diffusion model framework (see Sestieri et al. 2014).

2.2.2. Stimulus selection

The stimuli consisted of 256 × 256 pixel color photographs depicting indoor and outdoor scenes belonging to different categories (e.g. forest, church). Most of the images have been used in our previous fMRI studies (Guidotti et al., 2020; Sestieri et al., 2014), and were originally selected from a large database (Konkle et al., 2010) (http://cvcl.mit.edu/MM). To increase the number of trials for the MEG analysis, we selected additional images from the original database and the web. A total of 560 different images were used, 35 for the practice session and 525 for the MEG experiment. The stimulus set for the MEG experiment included 6 exemplars from 75 categories ($N = 450$) plus 1 exemplar from a different set of 75 categories (see Fig. 1A for an example).

The images in each category were selected based on a measure of physical similarity using the Matlab function "ssim", which evaluates image similarity based on the combination of three parameters (luminance, contrast, and structure). The similarity index was estimated for different spatial offsets across the image pairs, to account for the different standpoints used to take the pictures, and the maximum value was retained for each image pair in a given category. For each category, we selected 6 images so that only two images were physically similar (mean value across categories = 0.56 ± 0.05, range = 0.48–0.64) whereas the similarity values for all the other image pairs in the category were very low (mean value across categories = 0.14 ± 0.02, range 0.11–0.18). This procedure ensured the specificity of the similarity manipulation described below.

To control for the specificity of the perceptual similarity between items from different conditions, stimuli were consistently assigned to a specific condition. This raises a potential issue related to the contribution of the stimulus intrinsic memorability to both the behavioral and neural results. However, the effect of intrinsic memorability was not expected to overcome the robust effect of the current experimental manipulation, also given the number and variety of stimuli in each condition.

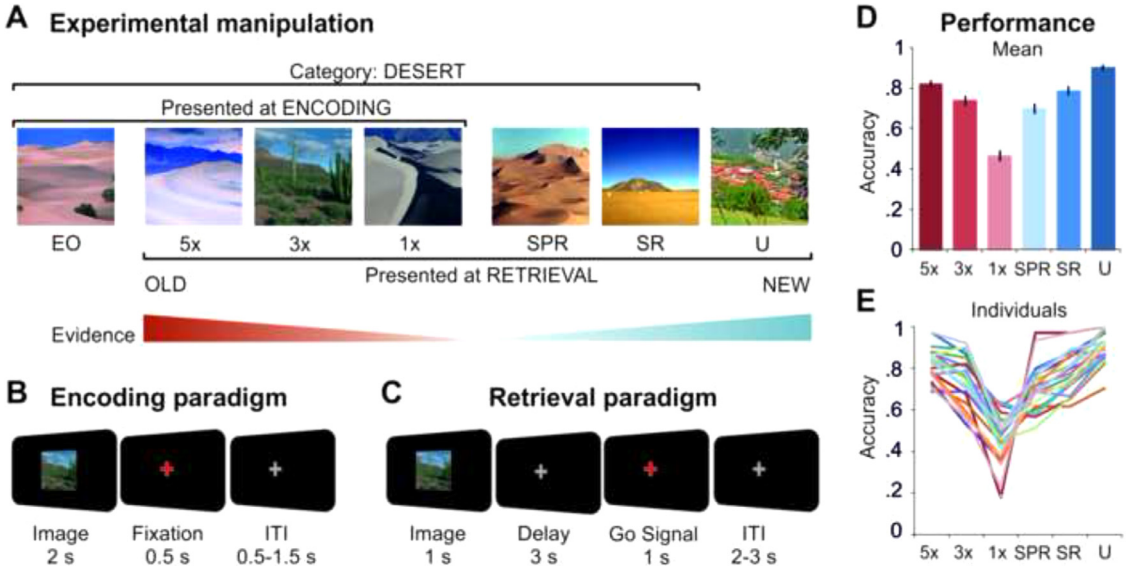

Fig. 1. Experimental paradigm. A. Example of the visual stimuli and the evidence manipulation. In the encoding session, four images depicting indoor or outdoor scenes for each of 75 categories ("desert" in the example) were presented at different frequencies (5x, 3x, 1x) to manipulate encoding strength. EO images were only presented once at encoding. At retrieval, old (previously encoded) images were characterized by increasing levels of evidence (5x = high, 3x = middle, 1x = low) toward old responses. Similarly, there were three types of new images (lures). SR and SPR images were selected from the same categories used in the encoding session: SR images were only semantically related to old images, whereas SPR images were also physically similar to EO images. Finally, U images were chosen from 75 new categories. The manipulation of similarity between old and new images created three levels of increasing evidence for new responses (*U* = high, SR = middle, SPR = low). Refer to Sections 2.2.3 and 2.2.4 for more explanations about the abbreviations. **B.** Trial structure of the encoding task. Each image was presented at the center of a black screen for 2 s, followed by a 500 ms red fixation cross. Participants were instructed to provide an indoor/outdoor judgment from the onset of the image until the offset of the red fixation cross. A variable ITI preceded the next trial. **C.** Trial structure of the retrieval task. Each image was presented at the center of a black screen for 2 s, followed by a gray fixation cross lasting for 3 s. Subjects were instructed to delay their judgment until the onset of the go signal, which was represented by the onset of a red cross lasting for 1 s. A variable ITI preceded the next trial. **D.** Mean retrieval accuracy across participants for the six experimental conditions. Error bars represent SEM. Participants exhibited an expected U-shape function, characterized by higher accuracy for high evidence compared with low evidence trials for both old (red) and new (blue) trials. **E.** Retrieval accuracy for each participant. Each line corresponds to an individual subject.

2.2.3. Encoding session

At encoding, subjects performed an incidental task (indoor/outdoor judgments) on visually presented images. Images belonged to 75 different categories, each including 4 exemplars. The four stimuli in each category were presented with different frequencies: two images were presented once ["1x" and encoding only ("EO") images], one was presented three times ("3x") and one was presented five times ("5x"). EO images were only presented at encoding and were specifically included for the manipulation of the physical similarity between old and new items at retrieval. A total of 15 blocks, each including 50 trials (5 1x, 5 EO, 15 3x, and 25 5x images), were presented. The order of stimulus presentation was the same for all subjects. Each trial started with the presentation of the image on a black background for 2 s, followed by a 500 ms red fixation cross (Fig. 1B). Subjects had a total of 2.5 s from the image onset to respond with the left or the right middle finger, depending on the specific judgment/response association (counterbalanced across subjects). A variable ITI (500–1500 ms) preceded the next trial. E-Prime 2 (Psychology Software Tools) was used for stimulus presentation and response collection.

2.2.4. Retrieval session

At retrieval, subjects performed item recognition decisions on old and new images (Fig. 1C). Old items (N = 225) included the whole set of 1x, 3x, and 5x images. A total of 225 new images were presented, divided into three types based on the evidence level toward new decisions: images belonging to 75 new categories, which were therefore unrelated ("U") to old images, images belonging to the same 75 categories used at encoding (semantically related, "SR"), and images belonging to the same categories and also physically similar to EO images ("SPR"). A total of 5 blocks, each including 90 trials, 15 for each of the six retrieval stimulus types, were presented. The order of stimulus presentation was the same for all subjects. Each trial started with the presentation of the image on a black background for 1 s, followed by a gray fixation cross (fixed delay) of 3 s. At the end of the delay, the fixation cross turned red for 1 s providing the go signal for the decision response. Subjects had 2 s from the onset of the go signal to provide an old/new judgment using the left or the right middle finger (the specific judgment/response association was counterbalanced across subjects). A variable ITI (2–3 s) followed the go-signal and preceded the next trial. E-Prime 2 (Psychology Software Tools) was used for stimulus presentation and response collection.

2.2.5. MEG recordings

MEG signals were recorded using a multi-channel MEG system installed in a magnetically shielded room at the University of Chieti, Italy (Della Penna et al., 2000; Pizzella et al., 2001). The MEG system consists of 153 dc SQUID magnetometers placed on a helmet-shaped surface covering the whole scalp. Magnetic fields were filtered in a 0.1–250 Hz band and continuously acquired at a 1025 Hz sampling rate. Two orthogonal electro-cardiographic and two orthogonal electro-oculographic channels were simultaneously recorded for offline artifact rejection. Stimuli were projected onto a screen situated inside the magnetically shielded room. Subjects responded using a LUMINA LU400 Response Pad (Cedrus Corporation). After each block, the subject's head position relative to the MEG sensors was estimated from the field produced by five coils placed on the scalp, whose positions were digitized together with anatomical landmarks. The anatomical reference used for MEG localization was obtained in each subject through a high-resolution structural MR image using a sagittal FFE T1-weighted sequence (TR = 8.14 ms, TE = 3.7 ms, flip angle = 8°, voxel size = 1 × 1 × 1 mm^3).

2.3. Behavioral data analysis

A repeated measure 2-way ANOVA with memory status (old, new) and evidence (low, middle, high) was conducted on response accuracy to test the effect of the experimental manipulation on behavioral performance. Tukey's tests were used for post-hoc analyses. We also coded trials in terms of signal detection theory by arbitrarily assigning the labels "HIT" and "MISS" to correctly and incorrectly identified old trials and the labels "correct rejection" (CR) and "false alarms" (FA) to correctly and incorrectly identified new trials. The HIT-FA difference was used to test brain-behavioral relationships.

2.4. MEG data analysis

2.4.1. MEG data preprocessing and ROI selection

The quality of MEG signals was inspected to remove time epochs with excessive noise (Larson-Prior et al., 2013). All trials including time intervals that failed the quality check were removed from the analysis. Then, signals were band-pass filtered in the 1–150 Hz band and were analyzed using a pipeline based on Independent Component Analysis to separate artifactual and brain components (ICs) at the sensor level (as in de Pasquale et al. (2021), Favaretto et al. (2021), Sebastiani et al. (2014), Spadone et al. (2021b)), (see Supplementary Materials for more details on ICA preprocessing). The sensor maps of the brain ICs were projected in the source space through a weighted minimum-norm least squares estimator implemented in Curry 6.0 (Neuroscan). This step was performed by segmenting the coregistered individual anatomical images to obtain a 3-compartment Boundary Element Method model. The individual source space consisted of a regular 3D grid within the innermost compartment of the head model, sampled through 4 mm side isotropic voxels (see Supplementary Materials for more details on source localization). The individual source maps were then transformed into the MNI152 reference system to enable across-subject analyses. Finally, the vector activities of each grid voxel were computed by linearly combining the brain IC time courses weighted by the related source maps.

For the time-frequency analysis, we converted a set of 165 centroids derived from an fMRI resting-state analysis (Baldassarre et al., 2014; Hacker et al., 2013) into a set of single MEG voxels (hereafter nodes). This procedure has been used in previous work (e.g., de Pasquale et al. 2021, Favaretto et al. 2021, Spadone et al. 2021b) as a way to cover the entire cortical sheet with a series of nodes corresponding to known resting-state networks: Dorsal-Attention, Ventral Attention, Somatomotor, Visual, Auditory, Language, Default Mode, FrontoParietal, Control. Four cerebellar nodes were deleted from the original set. MEG activity from single voxels is supposed to be virtually free from artifacts since the specific preprocessing pipeline used in the present study, based on ICA, linearly combined only identified brain components (removing both noise components and residual ICs). As a test of the spatial distribution of the effects, we conducted a control analysis on 27 neighboring voxels surrounding nodes exhibiting significant modulations in the main analysis (See Suppl. Figs. 2 and 3).

2.4.2. Time-frequency analysis

The average number of clean trials that were used in the time-frequency analysis is 53+/−9 across conditions (mean ± SD). We analyzed the power modulations in an epoch starting at −0.5 s and ending after 4 s from the onset of the image to identify the effect of the decision during memory retrieval in the large set of 165 nodes. Before running the time-frequency analysis, the average evoked activity was adaptively removed to extract the non-phase-locked rhythms from each condition and orthogonal direction of the vector activity (Capotosto et al., 2015; Favaretto et al., 2021; Spadone et al., 2017, 2021b). Next, the power spectrum density was estimated as a function of time and frequency using Morlet wavelets for each trial, activity direction, node, and subject. The frequencies ranged from 1 to 100 Hz with a 1 Hz frequency bin and a 1 ms temporal bin. The width of the wavelet expressed in the number of cycles varied as a linear function of frequency, according to the formula $\text{width} = 7 + \frac{\text{frequency}-10}{4}$ (Spadone et al., 2021a). These parameters were selected to set the width at about 7 in the alpha band, as this value corresponds to a good balance between temporal and frequency resolutions (Jensen et al., 2002), and to ensure this balance to the whole frequency interval. Then, the time-frequency representations of the power spectrum density were summed across the three directions of the vector activity for each node and averaged across trials of the same condition. Finally, the event-related desynchronization/ synchronization (ERD/ERS) as a function of time and frequency was computed as the instantaneous percentage power variation from the onset of image presentation (E) compared to the mean power in a baseline period (R) of 300 ms before the image onset, according to $\text{ERD/ERS}(t,f)(\%) = \frac{E(t,f)-R(f)}{R(f)} * 100$. The choice of the baseline period was motivated by the intention to minimize the risk of including the post-movement ERS of the preceding trials (see Supplementary Materials for a control analysis using a different baseline period). An example of the power modulation for each experimental condition, averaged across subjects and representative parietal nodes, is presented in Fig. 2B.

We then analyzed parameters describing the ERD/ERS dynamics at the individual level. For each subject and condition, we first identified the most responsive frequency as the one where the ERD/ERS peak occurred, within each physiological band [theta (4–8 Hz), alpha (8–15 Hz), low-beta (15–26 Hz), high-beta (26–35 Hz), low-gamma (35–50 Hz), high-gamma (50–100 Hz)]. The frequency boundaries defining the physiological bands were chosen according to guidelines from the HCP manual (see https://www.humanconnectome.org/storage/app/media/documentation/s1200/HCP_S1200_Release_Reference_Manual.pdf for details). Importantly, since we had no prior hypothesis on the precise timing of the decision-related modulations and we expected the presence of inter-subject variability, we applied a completely data-driven procedure (Spadone et al., 2021a), which automatically searched for the temporal and spectral position of the maximum ERD/ERS within each band excluding potential noise-related power modulations. First, we excluded the final part (1 s) of the epoch from the ERD/ERS peak searching algorithm, as this period might be affected by motor preparation. To account for the noise intrinsic in the power estimation, especially for conditions associated with a low number of trials, we applied an adaptive threshold for each frequency band instead of identifying the absolute minimum/maximum ERD/ERS. This threshold was used as the lower/upper limit to search for the first local ERD/ERS peak, which could also not correspond to the absolute minimum/maximum ERD/ERS. We assumed that the threshold was equal to the maximum relative error on the ERD/ERS peak, multiplied by the peak value. Thus, we estimated the relative error of the power spectrum density in the baseline epoch and we propagated it on the ERD/ERS formula $\text{THR} = (1 - \frac{\text{relERD/ERS}}{100}) \cdot |\text{ABS\_M}|$ (Spadone et al., 2021a).

Then, for each ERD/ERS peak detected with this procedure, we identified the onset and the offset of ERD/ERS at the responsive frequency, as the time in which the power modulation started and ended, respectively. These parameters were used to estimate the *area* under the curve from the onset to the offset of the ERS/ERD calculated with the trapezoidal method. The area can be considered a more stable measure of ERD/ERS strength in an experimental condition compared to the peak amplitude, which relies only on a value at a single time point. This parameter is conceptually similar to the calculation of the mean amplitude in a specific time interval but has the advantage of a data-driven estimation of the relevant interval. Compared to the method developed by (Maris and Oostenveld, 2007), the current procedure is not based on the identification of time points where a consistent power-related modulation is observed across subjects but rather automatically accounts for inter-subjects and inter-trial differences in the ERD/ERS dynamics.

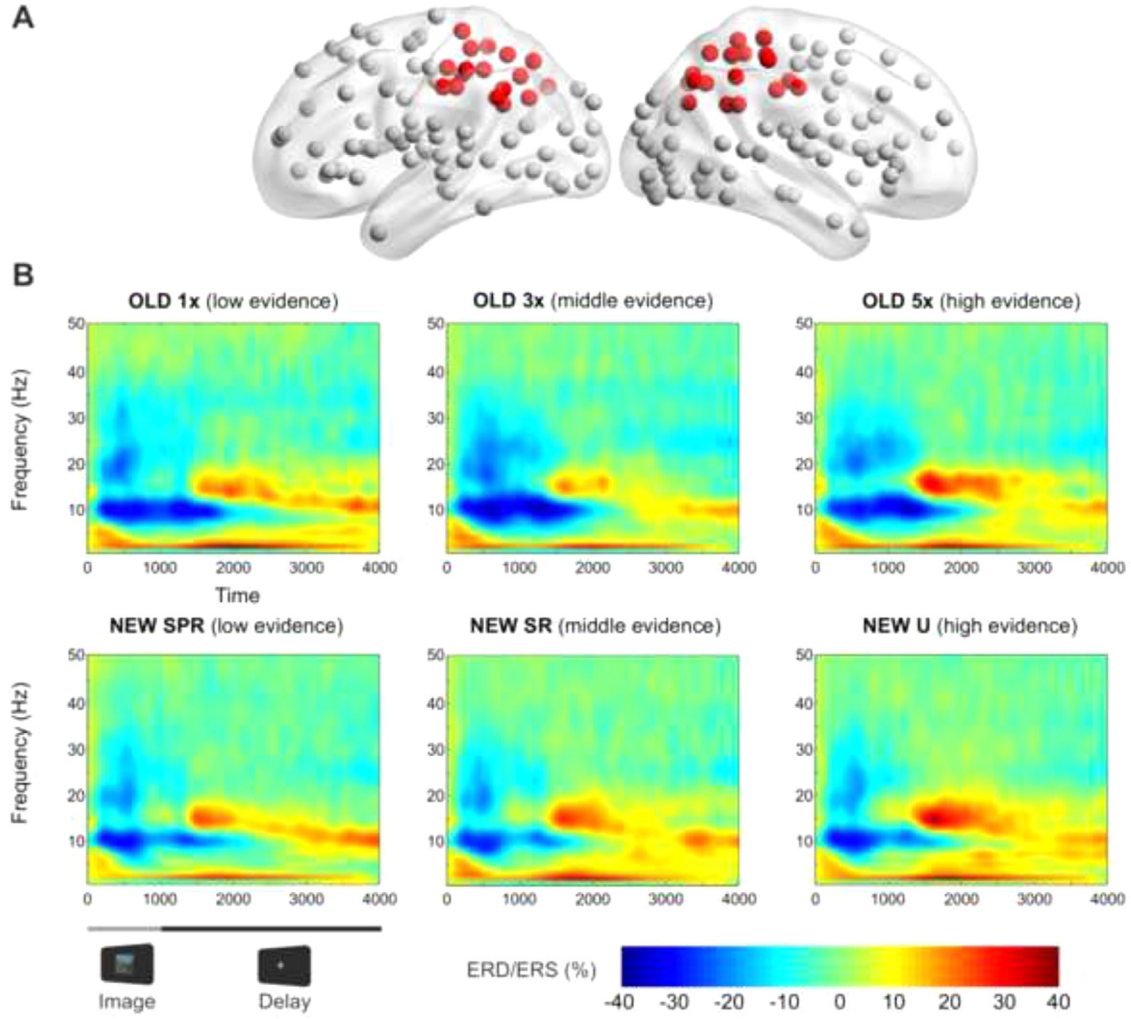

Fig. 2. Scalograms of retrieval-related activity in the parietal cortex. A. Illustration of the extended set of 165 nodes used for the time-frequency analyses, created using the centroids of a set of 169 fMRI ROIs representing nine well-characterized resting-state networks covering the whole brain (Baldassarre et al., 2014; Hacker et al., 2013). Nodes are displayed as spheres on a standard brain in lateral and dorsal views using a network visualization tool (Xia et al., 2013). The parietal nodes used for the scalograms are highlighted in red. **B.** Scalograms illustrating the retrieval-related activity for each level of evidence (columns) and memory status (rows) averaged across the parietal nodes. The scalograms terminate at the end of the delay phase, before the go signal onset.

2.4.3. Conjunction analysis

We first applied a set of analyses on the 165 nodes to identify regions where oscillatory activity showed a combination of retrieval success (HITs vs. CRs) and decision evidence (low vs. high evidence HITs) effects, looking at differences in ERS/ERD area. Since the behavioral results (see Section 3.1) indicated a significant difference in behavioral performance for old vs. new trials at extreme levels of evidence (low, high), the analysis of the retrieval success effect focused on the intermediate evidence level (middle). As no difference in task accuracy was observed in this condition, this procedure ensured that eventual old/new effects at the neural level did not reflect differences in behavioral performance. To avoid statistical dependencies between contrasts and maximize sensitivity, the effect of decision evidence was instead based on the comparison between the extreme evidence conditions (low, high). To take into account the possibility that regions involved in episodic memory retrieval show a greater or selective evidence effect on old compared to new trials, in this first step we limited the analysis to old trials (HITs), while the effect on new trials (CRs) was assessed in subsequent analyses (see Section 2.4.4).

The presence of a significant effect in both analyses was assessed through two-sample t-tests in each node and frequency band. To identify ROIs showing both effects, we estimated the probability of the two independent events as the product of the probability of each test (conjunction analysis). The resulting significance level was Bonferroni corrected by the number of regions ($N = 165$) in each frequency band. Finally, to gather information about the timing of retrieval success effects on the ERD/ERS area, we applied a *t*-test across subjects to the power modulation for HITs and CRs at each time point.

2.4.4. Additional regional analyses

A series of analyses were conducted on the nodes identified in the previous step to further investigate their role in the representation of a decision variable during item recognition. Firstly, we tested for the presence of an effect of evidence also on new trials, by comparing the ERS/ERD area in the extreme evidence conditions. Furthermore, we conducted a series of analyses to better characterize the ERD/ERS temporal dynamics that distinguished trials with different levels of decision evidence. In particular, based on the hypothesis that higher evidence trials should be associated with a steeper and faster accumulation process compared to lower evidence trials (Smith and Ratcliff, 2004), we tested whether the evidence effect in the absolute ERD/ERS area was explained by a difference in ERD/ERS *duration* and or in *peak amplitude*. Specifically, whereas ERD/ERS *duration*, i.e., the difference between the offset and the onset of the power modulation at the responsive fre-

quency, represents a measure of processing time (Spadone et al., 2021a), peak *amplitude* represents a standard measure of neuronal recruitment (Pfurtscheller, 2001). Therefore, for each ERD/ERS parameter and node of interest, we performed a *t*-test comparing low and high evidence conditions across participants, separately for HITs and CRs trials.

Secondly, we examined whether the inter-subject variability in the retrieval success effect showed a co-variation with the inter-subject variability in behavioral performance. To this aim, we conducted a Spearman correlation test between the old vs. new difference in ERD/ERS area (intermediate evidence level, correct trials) and the HIT-FAs difference, which represents an index of individual sensitivity.

Finally, we used a within-subject classification approach to test whether the measure of ERD/ERS area better predicts the objective memory status of the probe or the subjective memory choice (independent from accuracy) using trials from the low evidence condition, where the two indices were maximally divergent (i.e., lowest performance). For each subject, we extracted a measure of the ERD/ERS area from 500 random blocks of 5/10/15/20 trials. Small groups of trials were averaged instead of obtaining single-trial estimates to enhance the signal-to-noise ratio (SNR), following a standard procedure in the ERD/ERS literature (Pfurtscheller and Lopes da Silva, 1999). The parameters extracted from the 500 blocks were used for the classification analysis. A Linear Support Vector Machine (SVM) was trained on 75% of the randomly selected blocks and tested on the remaining blocks. The procedure was repeated 1000 times and the average classification accuracy was assigned to each subject. The values obtained for the objective memory status of the probe and the subjective memory decision were compared using paired t-tests across subjects.

3. Results

3.1. Behavioral results

As expected, the two-way ANOVA on response accuracy with memory status (old, new) and evidence (low, middle, high) as factors revealed a robust effect of evidence [$F(2, 42) = 386.64$, $p < 0.0001$]. The analysis also indicated a significant main effect of memory status [$F(1, 21) = 14.38$, $p < 0.001$] and a significant interaction effect [$F(2, 42) = 27.15$, $p < 0.0001$]. Accordingly, as displayed in Fig. 1D, while the evidence manipulation affected both old and new trials, performance was generally higher for new vs. old trials and the difference was most evident in low evidence trials. The low behavioral performance for old trials was somewhat unexpected, as it was not observed in our previous study using a very similar paradigm (Sestieri et al., 2014). However, it was probably due to the increased number of trials per condition ($N = 75$) that were necessary to have sufficient power forthe MEG time-frequency analysis. The presence of a significant effect of evidence on both new and old decisions, which was an important prerequisite for subsequent analyses, was additionally confirmed by post-hoc tests (Tukey) indicating a significant difference between 1x, 3x, and 5x trials (all $p < 0.001$) and between SPR, SR, and U images (all $p < 0.001$). The post-hoc tests also showed a significant difference between performance during old and new trials at low ($p < 0.001$) and high evidence levels ($p < 0.005$) but not during old and new trials at intermediate evidence levels (p = n.s.).

3.2. Alpha-rhythm modulations are sensitive to retrieval success and decision evidence

Fig. 2 illustrates the scalograms averaged across subjects for each experimental condition and extracted from a representative set of parietal nodes. From individual scalograms, separate conjunction analyses were performed on ERD/ERS area in each frequency band [theta (4–8 Hz), alpha (8–15 Hz), low-beta (15–26 Hz), high-beta (26–35 Hz), low-gamma (35–50 Hz), high-gamma (50–100 Hz)]. For conciseness, we only present the results in the alpha band, in which at least one node showed a significant conjunction effect after Bonferroni correction. Importantly, no significant conjunction effect survived correction for multiple comparisons in other frequency bands.

Fig. 3A illustrates the brain nodes showing a significant old/new difference in the absolute value of the alpha ERD area when comparing the two intermediate evidence levels across subjects.

The effect of retrieval success was widespread and particularly evident in frontal and parietal regions and was characterized by a larger alpha ERD in the old condition across all the brain nodes considered in the analysis. In contrast, the observed modulation by decision evidence on the absolute alpha ERD area (Fig. 3B) was much more focally distributed. Crucially, it was mainly observed in the left lateral parietal cortex, with the low evidence level associated with a larger absolute ERD area compared to the high evidence level. A similar, albeit weaker, effect was observed in the left insula and the right precuneus. The conjunction analysis indicated that only three nodes of the left PPC, located in the left IPS, AG, and IPL (red spheres in Fig. 2C), showed a combination of retrieval success and decision evidence effects on the ERD/ERS area.

Fig. 4 shows a close examination of the dynamics of the alpha ERD in IPS and AG (similar waveforms were observed in IPL, see Suppl. Fig. 1A). The post-hoc analysis indicated that the significant old-new effect in the IPS [$t = 2.9$, $p < 0.01$] started around 400 ms after the onset of the probe stimulus and lasted for approximately 2 s. While the onset of the ERD modulation is in line with previous reports (e.g., Martin-Buro et al. 2020) and more in general with the parietal old/new effect also described in the ERP literature (Rugg and Curran, 2007), the duration of the effect likely reflects the particular delay paradigm employed in the current study. A similar effect was observed in the IPL (Suppl. Fig. 1A) [$t = 2.5$; $p < 0.05$] and AG (Fig. 4B) [$t = 2.7$, $p < 0.05$], although in this case a significant divergence between the time courses was often not present at the level of individual time points. The analysis of the modulatory effect by decision evidence (high vs. low) for old decisions indicated the presence of a significant effect in the IPS [$t = 2.4$, $p < 0.05$, Fig. 4C], the AG [$t = 2.8$, $p < 0.01$, Fig. 4D] and the IPL ($t = 2.7$, $p < 0.01$, Suppl. Fig. 1B). A control time-frequency analysis was conducted on 162 voxels, partly surrounding the IPS and AG nodes and partly along a spatial trajectory linking IPS with AG, to examine the spatial distribution of the effects found in these regions (see Suppl. Fig. 2). The analysis demonstrated that the effects were not observed in single isolated voxels and that signals from the two sources (IPS and AG, which are about 3 cm apart) were distinguishable.

3.3. Effects of decision evidence on ERD/ERS temporal dynamics

Once we identified nodes modulated by retrieval success and decision evidence for old trials, we examined whether they were also sensitive to the amount of evidence for new decisions. A significant modulation of decision evidence on alpha ERD area was found in the IPS [$t = 3.3$, $p < 0.005$] and in the IPL [$t = 2.8$, $p < 0.01$] but not in the AG [$t = 0.9$, p = n.s.]. Then, a series of additional analyses were conducted to better characterize the temporal dynamics of alpha ERD in different evidence conditions. In particular, we tested whether the manipulation of decision evidence affected alpha ERD *duration*, a more specific index of processing time, in addition to absolute alpha ERD area, in the three nodes of interest. Fig. 5A shows that the difference in the duration of the alpha ERD was significant in the IPS node for both old and new correctly identified trials [HIT: $t = 2.4$, $p < 0.05$; CR: $t = 2.1$, $p < 0.05$], with higher evidence trials associated with a shorter ERD duration. The figure also qualitatively suggests the presence of a parametric effect across the three evidence levels for both old and new trials, although a statistically significant difference was only observed between extreme evidence levels. In contrast, the alpha ERD duration in the AG node was significantly modulated by decision evidence in old trials [$t = 3.2$, $p < 0.005$] but not in new trials [$t = 0.3$, p = n.s.] (Fig. 5B), where conditions were also not properly ordered. No significant evidence related differences

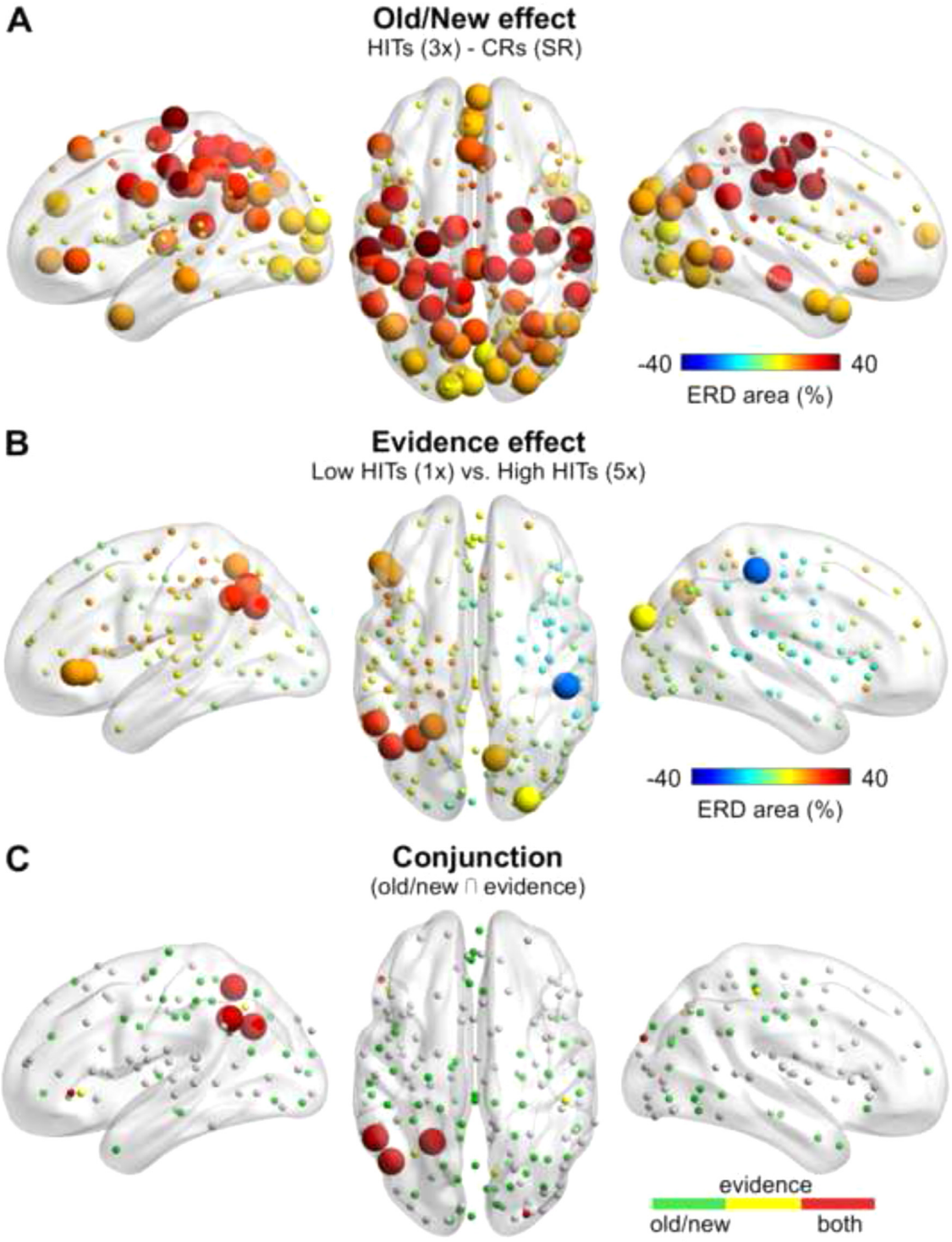

Fig. 3. Conjunction analysis of old/new and evidence effects. A. Uncorrected map of brain nodes showing a significant old/new effect (retrieval success) in the alpha ERD area at the intermediate evidence level. Yellow to red colors represent greater absolute alpha ERD area for old trials (HITs) whereas light to dark blue colors indicate greater absolute alpha ERD area for new trials (CRs). A larger sphere size indicates a significant *t*-test across subjects at $p < 0.05$. **B.** Uncorrected map of brain nodes showing a significant evidence effect (low vs. high) for old trials in the absolute alpha ERD area. Yellow to red colors represent greater alpha ERD for low evidence trials (1x) whereas light to dark blue colors indicate greater alpha ERD for high evidence trials (5x). **C.** Conjunction analysis to highlight brain nodes showing both effects. A different color is assigned to each node depending on whether it exhibits a significant retrieval success (green), a significant evidence effect (yellow), or both effects (red). To identify nodes showing a reliable conjunction effect (big spheres), we first combined the probability of the two independent events using the product of the probability of the null hypothesis of each test and then corrected for multiple comparisons ($N = 165$) using a Bonferroni approach.

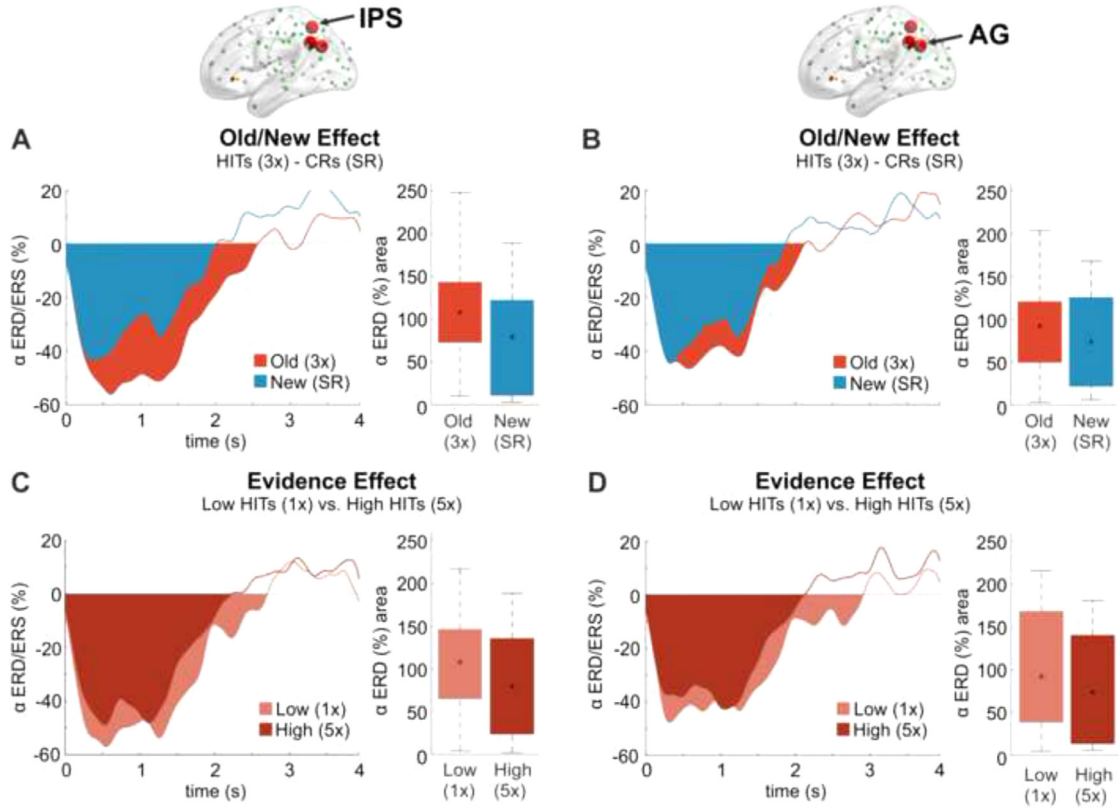

Fig. 4. Waveforms of alpha ERD from parietal nodes showing a significant conjunction effect. A and B. Group-average waveforms of alpha ERD starting at image onset for correct old (red) and new (blue) trials at the intermediate evidence level extracted from two parietal nodes (IPS, AG) identified in the conjunction analysis. The box plots on the right of each waveform represent the average alpha ERD area across subjects. Note that the group-average ERD area extracted from the average waveform across subjects (shown for graphical purposes) does not necessarily correspond to the average of the same ERD property extracted from single subjects (box plots), which was used to compute the statistics. **C** and **D.** Group-average waveforms of alpha ERD for low (light red) and high (dark red) evidence old trials extracted from the same nodes and box plots representing the mean and the standard error of the alpha ERD area across subjects in the same experimental conditions.

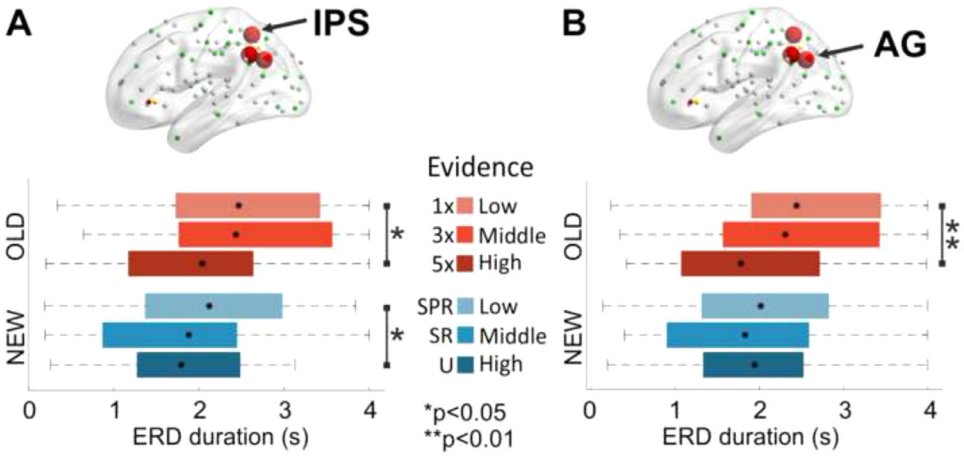

Fig. 5. Effect of decision evidence on alpha ERD duration. A and B. Box plots representing the average alpha ERD duration across subjects for the six experimental conditions in the IPS (A) and AG (B) nodes. In the IPS, low evidence trials triggered a more prolonged ERD than high evidence trials for both old and new trials, whereas a significant difference was only observed for old trials in the AG. The intermediate evidence condition was not considered in the statistical analysis but indicates a parametric variation of alpha ERD duration across the three levels of evidence in the IPS.

were observed for the alpha ERD duration in the IPL node [HIT: $t = 1.9$, p = n.s.; CR: $t = 1.6$, p = n.s., Suppl. Fig. 1C]. Again, a control analysis conducted on 162 voxels located around the IPS and AG nodes and along a spatial trajectory linking IPS with AG confirmed the presence of a clear anatomo-functional distinction.

Similar analyses were also conducted to test whether the effect on absolute alpha ERD area was also associated with an effect on peak amplitude, a traditional index of neuronal recruitment. For the IPS node, a significant difference between high and low evidence conditions was found only for HITs ($t = 2.8$, $p < 0.05$) but not for CRs ($t = 1.7$, p = n.s.). A similar pattern was found for the IPL node [HIT: $t = 2.2$, $p < 0.05$; CR: $t = 1.8$, p = n.s.] whereas no significant difference was observed for the AG [HIT: $t = 1.8$, p = n.s.; CR: $t = 0.8$, p = n.s.]. Overall, the results indicate that a consistent evidence effect across old and new trials was only observed for alpha ERD duration in the IPS. As hypothesized, higher evidence trials were associated with shorter ERD duration.

3.4. *Further indices of decision-related activity in IPS*

We next tested whether the pattern of oscillatory modulation in these nodes was associated with behavioral performance across subjects. Specifically, we hypothesized that if the difference in the ERD/ERS area

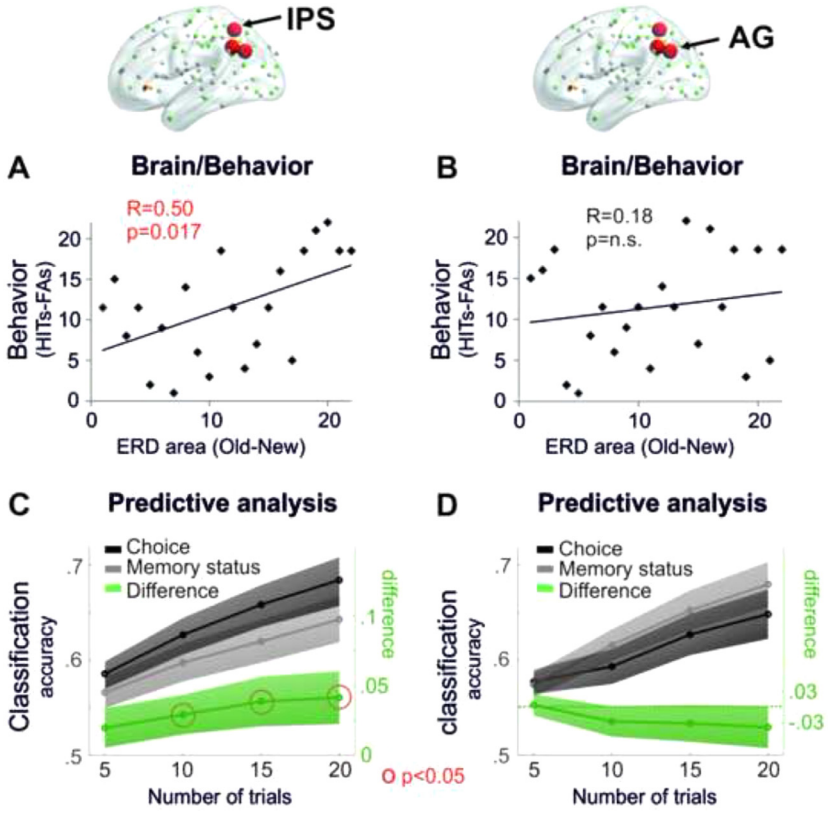

Fig. 6. Relationship with behavioral performance. A and B. Scatterplots of the relationship across subjects between the retrieval success effect (old/new effect at the intermediate evidence level) in the alpha ERD area extracted from the IPS (A) and the AG (B) and the accuracy of item recognition at the intermediate evidence level, calculated as the difference between the number of HITs and FAs. Both measures are expressed in ranks. A significant Spearman correlation ($p < 0.05$) is observed selectively in the IPS, suggesting that the individual ability to differentiate between old and new trials is related to the difference in alpha ERD elicited by the two trial types in this region. **C** and **D.** The graphs show the ability to predict the trial type using a classification approach on the measure of the alpha area recorded in the IPS (**C**) and AG (**D**) nodes. The dark and light gray lines represent the accuracy of the classification of the subjective memory choice (independent of accuracy) and the objective memory status of the probe (independent of the response), respectively. Values of alpha ERD were extracted from the low evidence level when the subjective choice and memory status were maximally divergent due to low recognition performance. The x-axis indicates the number of the small groups of trials that were averaged to increase SNR and train the classifier. The green line represents the difference between the classification accuracy obtained with the two analyses and the red circle indicates a significant difference at $p < 0.05$ (paired *t*-test across subjects). A significantly better prediction of choice compared to memory status is already observed in the IPS node when using blocks of 10 trials and increases as a function of block numerosity, suggesting that alpha ERD in this node tracks the subjective impression that the item is old or new. No significant result is observed in the AG, where a difference is even observed in the opposite direction.

between old and new judgments reflects the subject's ability to decide between the two outcomes, then subjects showing a greater modulation in the ERD/ERS area should also exhibit a greater modulation of performance at the memory decision task. Notably, a significant correlation between the individual recognition accuracy (HIT-FAs) and the retrieval success effect in the alpha ERD area was observed in the IPS [rho = 0.50, $p < 0.05$, Fig. 6A] but not in the IPL [rho = −0.02, p = n.s.] or in the AG [rho = 0.18, p = n.s., Fig. 6B] nodes.

Finally, a classification approach was applied to the analysis of the ERD/ERS area in the identified regions to test the hypothesis that decision-related activity better tracks the subjective rather than the objective memory status. As expected based on SNR, the ability to predict the memory choice and the memory status from the alpha ERD area increased in all the nodes of interest as a function of the number of trials used to compute ERD parameters and train the classifier (Fig. 6C, D). Crucially the classification of the subjective memory choice in the IPS node consistently outperformed that of the objective memory status (all ps < 0.05, Fig. 6C), except for the condition with the lowest SNR, suggesting that the alpha ERD in this region better tracked the subject's decision (subjective choice) rather than the item history (objective memory status). A different pattern was observed in the AG (Fig. 6D) and the IPL (Suppl. Fig. 1D) nodes, where no significant differences were observed between the classification of memory choice and memory status, regardless of SNR (all ps = n.s.).

4. Discussion

The present study tested the hypothesis that alpha desynchronization in the parietal lobe encodes decision-related signals during memory retrieval. We identified a region of the IPS where the pattern of alpha ERD was modulated by both retrieval success and the amount of decision evidence. Notably, the effect of evidence in this node was observed for both old and new trials and also involved the duration of the alpha ERD. Alpha ERD in IPS was also behaviorally relevant, as demonstrated by the significant covariation between the effect on ERD area and task performance across subjects. A classification analysis further indicated that the alpha ERD area in IPS better tracked the subjective memory judgment than the objective memory status, supporting a role in the representation of a decision variable during memory retrieval. The spatial and functional specificity of the present findings provide support for a recent anatomical-functional model of the parietal involvement in episodic memory retrieval (Sestieri et al., 2017) and characterize the alpha ERD as a potential marker of the hypothesized evidence accumulation process during memory-based decisions.

4.1. Parietal alpha ERD and the mnemonic accumulator hypothesis

The mnemonic accumulator hypothesis (Wagner et al., 2005) originates from two main lines of evidence: the pattern of BOLD activity in the parietal lobe during memory retrieval, which is compatible with decisional aspects of the task (e.g., Kahn et al. 2004, Wheeler and Buckner 2003), and the results of classical neurophysiological investigations of perceptual decision making in awake behaving monkeys (Gold and Shadlen, 2007). In particular, during perceptual decisions, the monkey lateral intraparietal (LIP) area is known to exhibit a ramp-like activity that matches the mechanism of evidence accumulation proposed by mathematical models of decision-making (e.g., Brown and Heathcote 2008, Ratcliff 1978, Usher and McClelland 2001). These models conceptualize decisions as a noisy accumulation of evidence for each option until the process reaches a threshold, after which the corresponding choice is executed. Importantly, also item recognition has been framed in terms of a process of evidence accumulation about the relatedness between probes and items present in the memory set (Ratcliff, 1978). This analogy offers the opportunity to think about the parietal retrieval-related activity as a manifestation of an accumulator process, whose strength contributes to the eventual memory decision. Importantly, the model predicts that the steepness, and thus the duration, of the accumulation process depends on the amount of evidence toward a specific decision

outcome. In a series of fMRI studies, we have provided additional evidence supporting a role for the IPS in memory-based decision-making, such as a sustained response whose duration scales with the length of cued recollection (Sestieri et al., 2011), a parametrical sensitivity to the amount of decision evidence during item recognition (Sestieri et al., 2014), and the ability to predict the subject's choices during both item recognition (Guidotti et al., 2020) and source memory (Guidotti et al., 2019) paradigms.

With the present study, we demonstrate that the alpha ERD in IPS shows several properties that are consistent with the fMRI literature and, more in general, with the mnemonic accumulator hypothesis. Firstly, the present alpha modulations in the IPS fit well with the topography of the aforementioned fMRI studies (Guidotti et al., 2019, 2020; Sestieri et al., 2014), especially when considering that the MEG analysis was data-driven over a large number of nodes spanning the entire cortical sheet, without any spatial constraint. Secondly, the sensitivity to retrieval success and, most importantly, to the amount of decision evidence for both old and new trials follows the prediction of a mnemonic accumulator. The sustained temporal profile observed during the delay period further supports a link with a gradual accumulation of evidence that leads to the preparation of an appropriate motor response. Finally, the stronger association with subjective choice compared to memory status supports the idea that the parietal alpha ERD reflects the subjective perception that the item was previously encountered rather than the actual recovery of information about the item, consistent with the so-called "perceived oldness" effect observed in fMRI studies (Kahn et al., 2004; Wheeler and Buckner, 2003).

4.2. Functional significance of alpha ERD

Alpha (and beta) power decreases have been reported in seminal EEG studies investigating the oscillatory dynamics during episodic memory retrieval (e.g., Klimesch 1999). Based on the view that links the alpha rhythm to active inhibition, an alpha ERD would represent a release from the suppression and a mechanism for selecting relevant information during item recognition (Jensen and Mazaheri, 2010; Klimesch, 2012). According to this account, phasic posterior alpha is typically interpreted as an index of cognitive load or effort and the modulation by decision evidence observed in the present study could potentially be consistent with this framework. As a matter of fact, the disambiguation between evidence accumulation vs. task difficulty modulations is one of the major experimental challenges in the neuroscience of decision-making. However, the overall pattern of results, including the sensitivity to memory status (old vs. new effect) even when difficulty was matched across conditions, the relationship between the old vs. new effect and behavioral performance, and, most importantly, the stronger association between alpha ERD and subjective judgments, compared to objective memory status, are difficult to reconcile with a basic load/effort account. Similar considerations apply to other attentional accounts of parietal memory retrieval effects. In particular, the attention-to-memory model (Cabeza et al., 2008; Ciaramelli et al., 2008) proposes that dorsal and ventral parietal regions are involved in orienting top-down and bottom-up attention to memories, respectively. While the top-down account makes a similar prediction to the aforementioned load/effort account, the bottom-up account makes an opposite prediction (more attentional capture and thus stronger activity for high evidence compared to low evidence old items) to the present findings. Moreover, concerning previous studies focusing on prestimulus alpha ERD as an index of attentional effort/focus (e.g., Sokoliuk et al. 2019), it has to be noted that the current analyses did not focus on preparatory activity but rather on peri/post-retrieval processes, induced by the presentation of the probe stimulus, during item recognition.

The results of a series of recent EEG/MEG studies have brought a renewed interest in retrieval-related desynchronizations, especially in the alpha band (Duzel et al., 2003; Griffiths et al., 2021, 2019; Karlsson et al., 2020; Khader and Rosler, 2011; Martin-Buro et al., 2020; Sutterer et al., 2019). According to a recent hypothesis (Hanslmayr et al., 2016, 2012), desynchronization at low frequencies would represent a reduction of synchrony across a large population of neurons, which in turn enables neural assemblies to express stimulus-specific codes (i.e., distinct memory representations). Such an increase in SNR would be obtained by either increasing the firing rate of relevant neurons or by reducing correlated noise in the neuronal assembly. While this mechanistic framework appears particularly appealing, the alpha ERD might also have additional roles during the retrieval of information from long-term memory. In particular, Martin-Buro and colleagues have recently reported a stepwise delay in the peak latency of the posterior alpha ERD associated with different mnemonic outcomes (Martin-Buro et al., 2020). Based on these findings, the authors have proposed that the alpha ERD might reflect the gradual accumulation of memory strength or mnemonic evidence (Wagner et al., 2005). The same authors, however, also propose an alternative interpretation of their results based on the notion of an episodic buffer (e.g., Baddeley 2000, Wagner et al. 2005, see also Treder et al. 2021, for a similar interpretation). Notably, although the results of Martin-Buro et al. (2020) and Treder et al. (2021) have several points in common with the current findings, in terms of frequency, spatial distribution, and timing of desynchronizations, some key methodological differences have to be highlighted. In particular, in the study by Martin-Buro et al. (2020), participants distinguished between new items, items simply recognized, and items for which they could also recall the associated word. The additional recall process involved in the last case determined a qualitative difference compared to simple recognition and emphasized the potential involvement of an episodic buffer. A similar argument applies to the cued recall paradigm by Treder et al. (2021), in which the episodic buffer is supposed to support the reinstatement of content-specific information. This choice of task design also guides their interpretation of the alpha ERD modulation in the parietal cortex, especially of its more ventral component. In contrast, our participants only distinguished between old and new items, the experimental manipulation being a quantitative variation of decision/mnemonic evidence (decision uncertainty). Since successful recognition might simply be based on a pattern completion mechanism, a weaker contribution of the episodic buffer was expected in our task.

4.3. An anatomo-functional distinction in the left lateral parietal lobe

The present study further indicated the presence of a functional distinction between different parietal regions showing alpha ERD during memory retrieval. In particular, out of the three nodes that were isolated with the conjunction analysis, only the IPS exhibited additional properties, i.e., sensitivity for the amount of evidence for new decisions, behavioral relevance, stronger association with subjective choices compared to objective memory status, that support the definition of a memory-based decision variable in the brain. This functional distinction is consistent with an existing anatomo-functional model of the parietal involvement in memory retrieval (Sestieri et al., 2017). According to this model, regions of the inferior parietal lobule, such as the AG, are more specifically involved in the representation of the retrieved content, whereas more dorsal regions of the IPS provide a greater contribution to memory-based decision-making. Accordingly, while the activity of more ventral parietal regions appears more consistent with an episodic memory account, the involvement of more dorsal regions better matches a mnemonic accumulation account. In this framework, it is not surprising that the AG is sensitive to the amount of evidence for old responses, since memory strength is usually positively associated with the quantity of retrieved information. On the other hand, as no or little information can be successfully recollected for new items, even when they resemble old materials, the same region is not expected to necessarily distinguish between levels of evidence for new responses. This pattern of activity is different from a decision-related region, which is instead expected to differentiate between levels of evidence for the decision, regardless of the behavioral outcome.

4.4. Oscillatory activity and accumulation signals

Although the present results are consistent with a decision-making account for the alpha ERD in IPS, they do not necessarily reflect the kind of evidence accumulation process (i.e., ramp-like activity) described in the monkey single-unit studies during perceptual decisions. Several studies have attempted to identify the EEG/MEG correlates of a putative accumulation mechanism, especially during perceptual decisions (e.g., Donner et al. 2009, Philiastides et al. 2014, Ratcliff et al. 2009, see also van Vugt et al. 2016, 2019) for similar approaches applied to short-term memory paradigms). The most promising candidate has been identified in the central parietal positive (CPP) ERP component, a supramodal signal that peaks at response latency and whose buildup rate scales with the amount of decision evidence (Kelly and O'Connell, 2013; Loughnane et al., 2016; O'Connell et al., 2012; Pisauro et al., 2017; van Vugt et al., 2019). However, several properties of the CPP do not easily fit with the literature on episodic memory retrieval. The first issue concerns the spatial localization of the effect. Besides the low spatial resolution of the EEG technique, the neural generator of the CPP has been localized in the medial prefrontal cortex (Pisauro et al., 2017), far from parietal regions showing retrieval-related effects (Sestieri et al., 2017; Wagner et al., 2005). Another issue is that the topography of the CCP suggests a primary involvement in action intention and response preparation, whereas previous data suggest relative independence between evidence accumulation and motor intention during memory retrieval (Sestieri et al., 2014; Shannon and Buckner, 2004). The same issue pertains also to the results of studies that have identified a magnetoencephalographic signature of evidence accumulation by looking a the dynamics of brain oscillations in sensorimotor regions (Donner et al., 2009; van Vugt et al., 2012). Indeed, some have even expressed doubts about the feasibility to track accumulation signals in the time/frequency domain during a memory task (van Vugt et al., 2016). In this respect, we note that an accumulation process occurring at the level of spiking activity of individual neurons does not necessarily translate to a modulation of oscillatory activity recorded in a large neuronal population, as recorded by MEG. Thus, while the present results allow the establishment of a clearer connection between the results of fMRI and MEG studies on memory retrieval, the gap between the results of decision-making studies conducted with intracranial and scalp neurophysiological techniques still poses a great challenge for the definition of general decision variables in the human brain.

5. Conclusions

The analyses of oscillatory activity in the alpha band confirm the presence of a functional subdivision between posterior parietal regions involved in memory retrieval and support the role of alpha ERD within the intraparietal sulcus in memory-based decision-making.

Declaration of Competing Interest

The authors declare no competing financial interests

Credit authorship contribution statement

Sara Spadone: Data curation, Formal analysis, Investigation, Methodology, Software, Visualization, Writing – original draft. **Annalisa Tosoni:** Conceptualization, Writing – review & editing. **Stefania Della Penna:** Conceptualization, Methodology, Software, Supervision, Writing – review & editing. **Carlo Sestieri:** Conceptualization, Funding acquisition, Supervision, Writing – original draft, Writing – review & editing.

Acknowledgment

We thank Roberto Guidotti for his technical help. This study was supported by a Bial Foundation Grant (#159-2016) to C.S. and by the "Departments of Excellence 2018–2022″ initiative of the Italian Ministry of Education, University and Research for the Department of Neuroscience, Imaging and Clinical Sciences (DNISC) of the University of Chieti-Pescara, and the Department of Neuroscience University of Padua.

Data/code availability statement

The empirical data used for this paper are available in the public repository "Mendeley Data" (https://data.mendeley.com/). The codes used for this paper are available upon request from the corresponding author.

Supplementary materials

Supplementary material associated with this article can be found, in the online version, at doi:10.1016/j.neuroimage.2022.119345.

References

Baddeley, A., 2000. The episodic buffer: a new component of working memory? Trends Cogn. Sci. 4, 417–423.
Baldassarre, A., Ramsey, L., Hacker, C.L., Callejas, A., Astafiev, S.V., Metcalf, N.V., Zinn, K., Rengachary, J., Snyder, A.Z., Carter, A.R., Shulman, G.L., Corbetta, M., 2014. Large-scale changes in network interactions as a physiological signature of spatial neglect. Brain 137, 3267–3283.
Brown, S.D., Heathcote, A., 2008. The simplest complete model of choice response time: linear ballistic accumulation. Cogn. Psychol. 57, 153–178.
Cabeza, R., Ciaramelli, E., Olson, I.R., Moscovitch, M., 2008. The parietal cortex and episodic memory: an attentional account. Nat. Rev. Neurosci. 9, 613–625.
Capotosto, P., Spadone, S., Tosoni, A., Sestieri, C., Romani, G.L., Della Penna, S., Corbetta, M., 2015. Dynamics of EEG rhythms support distinct visual selection mechanisms in parietal cortex: a simultaneous transcranial magnetic stimulation and EEG study. J. Neurosci. 35, 721–730.
Ciaramelli, E., Grady, C.L., Moscovitch, M., 2008. Top-down and bottom-up attention to memory: a hypothesis (AtoM) on the role of the posterior parietal cortex in memory retrieval. Neuropsychologia 46, 1828–1851.
de Pasquale, F., Spadone, S., Betti, V., Corbetta, M., Della Penna, S., 2021. Temporal modes of hub synchronization at rest. Neuroimage 235, 118005.
Della Penna, S., Del Gratta, C., Granata, C., Pasquarelli, A., Pizzella, V., Rossi, R., Russo, M., Torquati, K., Erné, S.N., 2000. Biomagnetic systems for clinical use. Philos. Mag. B 80, 937–948.
Donner, T.H., Siegel, M., Fries, P., Engel, A.K., 2009. Buildup of choice-predictive activity in human motor cortex during perceptual decision making. Curr. Biol. 19, 1581–1585.
Duzel, E., Habib, R., Schott, B., Schoenfeld, A., Lobaugh, N., McIntosh, A.R., Scholz, M., Heinze, H.J., 2003. A multivariate, spatiotemporal analysis of electromagnetic time-frequency data of recognition memory. Neuroimage 18, 185–197.
Favaretto, C., Spadone, S., Sestieri, C., Betti, V., Cenedese, A., Della Penna, S., Corbetta, M., 2021. Multi-band MEG signatures of BOLD connectivity reorganization during visuospatial attention. Neuroimage 230, 117781.
Gold, J.I., Shadlen, M.N., 2007. The neural basis of decision making. Annu. Rev. Neurosci. 30, 535–574.
Griffiths, B.J., Martin-Buro, M.C., Staresina, B.P., Hanslmayr, S., Staudigl, T., 2021. Alpha/beta power decreases during episodic memory formation predict the magnitude of alpha/beta power decreases during subsequent retrieval. Neuropsychologia 153, 107755.
Griffiths, B.J., Mayhew, S.D., Mullinger, K.J., Jorge, J., Charest, I., Wimber, M., Hanslmayr, S., 2019. Alpha/beta power decreases track the fidelity of stimulus-specific information. Elife 8, e49562. doi:10.7554/eLife.49562.
Guidotti, R., Tosoni, A., Perrucci, M.G., Sestieri, C., 2019. Choice-predictive activity in parietal cortex during source memory decisions. Neuroimage 189, 589–600.
Guidotti, R., Tosoni, A., Sestieri, C., 2020. Properties and temporal dynamics of choice- and action-predictive signals during item recognition decisions. Brain Struct. Funct. 225, 2271–2286.
Hacker, C.D., Laumann, T.O., Szrama, N.P., Baldassarre, A., Snyder, A.Z., Leuthardt, E.C., Corbetta, M., 2013. Resting state network estimation in individual subjects. Neuroimage 82, 616–633.
Hanslmayr, S., Staresina, B.P., Bowman, H., 2016. Oscillations and episodic memory: addressing the synchronization/desynchronization conundrum. Trends Neurosci. 39, 16–25.
Hanslmayr, S., Staudigl, T., Fellner, M.C., 2012. Oscillatory power decreases and long-term memory: the information via desynchronization hypothesis. Front. Hum. Neurosci. 6, 74.
Jensen, O., Hari, R., Kaila, K., 2002. Visually evoked gamma responses in the human brain are enhanced during voluntary hyperventilation. Neuroimage 15, 575–586.
Jensen, O., Mazaheri, A., 2010. Shaping functional architecture by oscillatory alpha activity: gating by inhibition. Front. Hum. Neurosci. 4, 186.
Kahn, I., Davachi, L., Wagner, A.D., 2004. Functional-neuroanatomic correlates of recollection: implications for models of recognition memory. J. Neurosci. 24, 4172–4180.

Karlsson, A.E., Wehrspaun, C.C., Sander, M.C., 2020. Item recognition and lure discrimination in younger and older adults are supported by alpha/beta desynchronization. Neuropsychologia 148, 107658.
Kelly, S.P., O'Connell, R.G., 2013. Internal and external influences on the rate of sensory evidence accumulation in the human brain. J. Neurosci. 33, 19434–19441.
Khader, P.H., Rosler, F., 2011. EEG power changes reflect distinct mechanisms during long-term memory retrieval. Psychophysiology 48, 362–369.
Klimesch, W., 1999. EEG alpha and theta oscillations reflect cognitive and memory performance: a review and analysis. Brain Res. Rev. 29, 169–195.
Klimesch, W., 2012. alpha-band oscillations, attention, and controlled access to stored information. Trends Cogn. Sci. 16, 606–617.
Konkle, T., Brady, T.F., Alvarez, G.A., Oliva, A., 2010. Scene memory is more detailed than you think: the role of categories in visual long-term memory. Psychol. Sci. 21, 1551–1556.
Larson-Prior, L.J., Oostenveld, R., Della Penna, S., Michalareas, G., Prior, F., Babajani-Feremi, A., Schoffelen, J.M., Marzetti, L., de Pasquale, F., Di Pompeo, F., Stout, J., Woolrich, M., Luo, Q., Bucholz, R., Fries, P., Pizzella, V., Romani, G.L., Corbetta, M., Snyder, A.Z., Consortium, W.U.M.H, 2013. Adding dynamics to the human connectome project with MEG. Neuroimage 80, 190–201.
Loughnane, G.M., Newman, D.P., Bellgrove, M.A., Lalor, E.C., Kelly, S.P., O'Connell, R.G., 2016. Target selection signals influence perceptual decisions by modulating the onset and rate of evidence accumulation. Curr. Biol. 26, 496–502.
Maris, E., Oostenveld, R., 2007. Nonparametric statistical testing of EEG- and MEG-data. J. Neurosci. Methods 164, 177–190.
Martin-Buro, M.C., Wimber, M., Henson, R.N., Staresina, B.P., 2020. Alpha rhythms reveal when and where item and associative memories are retrieved. J. Neurosci. 40, 2510–2518.
Nyhus, E., Curran, T., 2010. Functional role of gamma and theta oscillations in episodic memory. Neurosci. Biobehav. Rev. 34, 1023–1035.
O'Connell, R.G., Dockree, P.M., Kelly, S.P., 2012. A supramodal accumulation-to-bound signal that determines perceptual decisions in humans. Nat. Neurosci. 15, 1729–1735.
Osipova, D., Takashima, A., Oostenveld, R., Fernandez, G., Maris, E., Jensen, O., 2006. Theta and gamma oscillations predict encoding and retrieval of declarative memory. J. Neurosci. 26, 7523–7531.
Pfurtscheller, G., 2001. Functional brain imaging based on ERD/ERS. Vis. Res. 41, 1257–1260.
Pfurtscheller, G., Lopes da Silva, F.H., 1999. Event-related EEG/MEG synchronization and desynchronization: basic principles. Clin. Neurophysiol. 110, 1842–1857.
Philiastides, M.G., Heekeren, H.R., Sajda, P., 2014. Human scalp potentials reflect a mixture of decision-related signals during perceptual choices. J. Neurosci. 34, 16877–16889.
Pisauro, M.A., Fouragnan, E., Retzler, C., Philiastides, M.G., 2017. Neural correlates of evidence accumulation during value-based decisions revealed via simultaneous EEG-fMRI. Nat. Commun. 8, 15808.
Pizzella, V., Della Penna, S., Del Gratta, C., Romani, G.L., 2001. SQUID systems for biomagnetic imaging. Supercond. Sci. Technol. 14, R79–R114.
Ratcliff, R., 1978. A Theory of Memory Retrieval. Psychol. Rev. 85, 59–108.
Ratcliff, R., Philiastides, M.G., Sajda, P., 2009. Quality of evidence for perceptual decision making is indexed by trial-to-trial variability of the EEG. Proc. Natl. Acad. Sci. USA 106, 6539–6544.
Ratcliff, R., Thapar, A., McKoon, G., 2004. A diffusion model analysis of the effects of aging on recognition memory. J. Mem. Lang. 50, 408–424.
Rugg, M.D., Curran, T., 2007. Event-related potentials and recognition memory. Trends Cogn. Sci. 11, 251–257.
Sebastiani, V., de Pasquale, F., Costantini, M., Mantini, D., Pizzella, V., Romani, G.L., Della Penna, S., 2014. Being an agent or an observer: different spectral dynamics revealed by MEG. Neuroimage 102, 717–728 Pt 2.
Sestieri, C., Corbetta, M., Romani, G.L., Shulman, G.L., 2011. Episodic memory retrieval, parietal cortex, and the default mode network: functional and topographic analyses. J. Neurosci. 31, 4407–4420.
Sestieri, C., Shulman, G.L., Corbetta, M., 2017. The contribution of the human posterior parietal cortex to episodic memory. Nat. Rev. Neurosci. 18, 183–192.
Sestieri, C., Tosoni, A., Mignogna, V., McAvoy, M.P., Shulman, G.L., Corbetta, M., Romani, G.L., 2014. Memory accumulation mechanisms in human cortex are independent of motor intentions. J. Neurosci. 34, 6993–7006.
Shannon, B.J., Buckner, R.L., 2004. Functional-anatomic correlates of memory retrieval that suggest nontraditional processing roles for multiple distinct regions within posterior parietal cortex. J. Neurosci. 24, 10084–10092.
Smith, P.L., Ratcliff, R., 2004. Psychology and neurobiology of simple decisions. Trends Neurosci. 27, 161–168.
Sokoliuk, R., Mayhew, S.D., Aquino, K.M., Wilson, R., Brookes, M.J., Francis, S.T., Hanslmayr, S., Mullinger, K.J., 2019. Two spatially distinct posterior alpha sources fulfill different functional roles in attention. J. Neurosci. 39, 7183–7194.
Spadone, S., Betti, V., Sestieri, C., Pizzella, V., Corbetta, M., Della Penna, S., 2021a. Spectral signature of attentional reorienting in the human brain. Neuroimage 244, 118616.
Spadone, S., Sestieri, C., Baldassarre, A., Capotosto, P., 2017. Temporal dynamics of TMS interference over preparatory alpha activity during semantic decisions. Sci. Rep. 7, 2372.
Spadone, S., Wyczesany, M., Della Penna, S., Corbetta, M., Capotosto, P., 2021b. Directed flow of beta band communication during reorienting of attention within the dorsal attention network. Brain Connect. 11 (9), 717–724.
Staresina, B.P., Wimber, M., 2019. A neural chronometry of memory recall. Trends Cogn. Sci. 23, 1071–1085.
Staudigl, T., Hanslmayr, S., 2013. Theta oscillations at encoding mediate the context-dependent nature of human episodic memory. Curr. Biol. 23, 1101–1106.
Sutterer, D.W., Foster, J.J., Serences, J.T., Vogel, E.K., Awh, E., 2019. Alpha-band oscillations track the retrieval of precise spatial representations from long-term memory. J. Neurophysiol. 122, 539–551.
Treder, M.S., Charest, I., Michelmann, S., Martin-Buro, M.C., Roux, F., Carceller-Benito, F., Ugalde-Canitrot, A., Rollings, D.T., Sawlani, V., Chelvarajah, R., Wimber, M., Hanslmayr, S., Staresina, B.P., 2021. The hippocampus as the switchboard between perception and memory. Proc. Natl. Acad. Sci. USA 118 (50). doi:10.1073/pnas.2114171118, e2114171118.
Usher, M., McClelland, J.L., 2001. The time course of perceptual choice: the leaky, competing accumulator model. Psychol. Rev. 108, 550–592.
van Vugt, M.K., Beulen, M.A., Taatgen, N.A., 2016. Is there neural evidence for an evidence accumulation process in memory decisions? Front. Hum. Neurosci. 10, 93.
van Vugt, M.K., Beulen, M.A., Taatgen, N.A., 2019. Relation between centro-parietal positivity and diffusion model parameters in both perceptual and memory-based decision making. Brain Res. 1715, 1–12.
van Vugt, M.K., Simen, P., Nystrom, L.E., Holmes, P., Cohen, J.D., 2012. EEG oscillations reveal neural correlates of evidence accumulation. Front. Neurosci. 6, 106.
Vilberg, K.L., Rugg, M.D., 2008. Memory retrieval and the parietal cortex: a review of evidence from a dual-process perspective. Neuropsychologia 46, 1787–1799.
Wagner, A.D., Shannon, B.J., Kahn, I., Buckner, R.L., 2005. Parietal lobe contributions to episodic memory retrieval. Trends Cogn. Sci. 9, 445–453.
Wheeler, M.E., Buckner, R.L., 2003. Functional dissociation among components of remembering: control, perceived oldness, and content. J. Neurosci. 23, 3869–3880.
Xia, M., Wang, J., He, Y., 2013. BrainNet viewer: a network visualization tool for human brain connectomics. PLoS One 8, e68910.